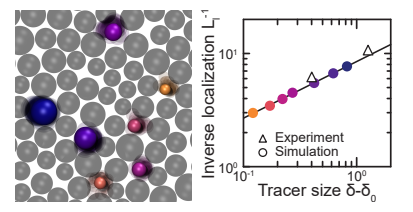
Structure Dominates Localization of Tracers Within Aging Nanoparticle Glasses

Ryan Poling-Skutvik, † Ryan C. Roberts, † Ali H. Slim, † Suresh Narayanan, ‡ Ramanan Krishnamoorti, † Jeremy C. Palmer, *, † and Jacinta C. Conrad*, † † Department of Chemical and Biomolecular Engineering, University of Houston, Houston, TX 77204-4004 † † Advanced Photon Source, Argonne National Laboratory, Argonne, IL 60439

Received March 26, 2019; E-mail: jcpalmer@uh.edu; jcconrad@uh.edu

Abstract: We investigate the transport and localization of tracer probes in a glassy matrix as a function of relative size using dynamic x-ray scattering experiments and molecular dynamics simulations. The quiescent relaxations of tracer particles evolve with increasing waiting time $t_{\rm w}$. The corresponding relaxation times increase exponentially at small $t_{\rm w}$ and then transition to a power-law behavior at longer $t_{\rm w}$. As tracer size decreases, the aging behavior weakens and the particles become less localized within the matrix until they delocalize at a critical size ratio $\delta_0\approx 0.38$. Localization does not vary with sample age even as the relaxations slow by approximately an order of magnitude, suggesting that matrix structure controls tracer localization.



Transport of small molecules, tracers, and particles within disordered glassy matrices can destabilize biological molecules in harsh environments, 1,2 govern the production of optically active nanoparticles, 3 affect the performance of membranes, 4,5 and introduce functionality in polymer nanocomposites. $^{6-12}$ In each scenario, understanding how matrix structure and dynamics 13 affect particle transport is essential for predicting the properties of these composite materials. Localization of particles within glasses, 14 for example, depends on particle size $^{15-17}$ as well as on void structure 18,19 and slow dynamics 16,20 of the matrix. Because tracer relaxations may occur on significantly shorter timescales than those of the matrix, this localization transition can exhibit strong similarities to dynamic arrest within a random matrix of immobile obstacles. $^{21-25}$

Fundamental understanding of tracer transport and localization within glassy matrices, however, is complicated by the fact that glasses age over time. Aging is a universal phenomenon in glasses, occurring in metallic and inorganic glasses, 26,27 polymers, 28 and colloids 29 and manifesting in macroscopic changes such as shrinkage 30 and increases in mechanical properties. 31 Microscopically, the dynamics in glasses evolve after the sample is quenched out-of-equilibrium, slowing and becoming more heterogeneous with aging time $t_{\rm w}$. $^{32-34}$ In the aging regime, heterogeneous stress relaxations 27,35 often lead to hyperdiffusive matrix dynamics. $^{36-38}$ Surprisingly, the mechanical and dynamical

changes occur with only minor changes in two-body metrics of matrix structure over time. 34,39,40 Although molecular 13 or particulate $^{40-43}$ tracers are commonly used to probe glassy behavior, how their dynamics depend on the structure and dynamics of the glassy matrix remains incompletely understood. An aging matrix whose dynamics evolve but whose structure remains effectively constant provides a model system by which to investigate the relative roles of matrix structure and dynamics on transport of tracer particles in heterogeneous complex media.

In this Letter, we investigate the transport and localization of tracer particles in aging glassy nanoparticle matrices, using x-ray photon correlation spectroscopy and eventdriven molecular dynamics (MD) to probe a complementary range of time scales. We characterize the dynamics of tracers whose size is smaller than or comparable to that of the matrix particles. In both experiment and simulation the tracer relaxations are hyperdiffusive, suggesting that tracers probe relaxation of internal stresses in the matrix. We observe two distinct aging regimes for both matrix and tracers, indicating that the relaxations of the tracers couple to those of matrix particles. The localization length quantifies the degree of coupling and decreases as the tracer to matrix particle size ratio δ is reduced. This length scale diverges at $\delta_0 \approx 0.38$, near the value at which tracers exhibit anomalous collective transport in glassy matrices, ^{16,20} but does not depend on matrix age. The lack of change in the localization length across a range of waiting times relative to relaxation time $10^{-4} \le t_{\rm w}/\tau \le 10^3$ suggests that structure strongly influences the transition from diffusion to localization in glassy materials, even though matrix relaxation enables anomalous diffusive transport of finite-sized tracers. By connecting tracer size to localization, we provide a basis from which to predict transport properties through slowly relaxing and heterogeneous materials.

Polystyrene particles (Thermo-Fisher Scientific) with diameter $\sigma = 60$ nm and polydispersity 10% were acquired as an aqueous suspension with volume fraction $\phi = 0.1$. Silica particles from nano Composix with nominal diameters $\sigma_{\rm nom}$ of 20 nm and 60 nm and polydispersities < 10% were acquired as aqueous suspensions with $\phi = 0.0023$ and 0.0046, respectively. To account for electrostatic repulsions, which modify the effective particle size, 44-46 we use the Barker-Henderson formalism to map the tracers onto a hard-sphere model (Supporting Information). This procedure yields effective hard sphere diameters of $\sigma_t = 47 \pm 4$ and 99 ± 2 nm for the nominally sized 20 and 60 nm tracers, respectively. Normalizing these hard-sphere sizes by the polystyrene matrix diameter gives $\delta \equiv \sigma_{\rm t}/\sigma = 0.78 \pm 0.06$ and 1.65 ± 0.03 , respectively. Polystyrene and silica suspensions were pipetted in appropriate ratios into an Amicon microcentrifuge filter tube

with a 10 kDa cutoff and centrifuged at $3000 \times g$ for 30 minutes. The centrifuge tube was then refilled with additional stock suspensions and centrifuged again to produce a glassy material near random close packing $(\phi \approx 0.64 \pm 0.03)^{47}$ (Supporting Information) with silica to polystyrene volume ratio of 0.002. Sample age is characterized by the waiting time $t_{\rm w}$, the elapsed duration from the end of centrifugation. The glassy sample was then placed into a 2-mm thick aluminum sample holder, sealed with Kapton windows to prevent evaporation, and attached to a copper block with Peltier to regulate temperature. Small-angle x-ray scattering (SAXS) indicated that the tracers were well dispersed in the glass (Supporting Information). X-ray photon correlation spectroscopy (XPCS) data were collected at a frame rate of $1 \, \mathrm{s}^{-1}$ on the 8 ID-I beamline at the Advanced Photon Source at Argonne National Laboratory over a wavevector range that depended on scattering intensity so that 0.003 $\mathring{\mathbf{A}}^{-1} \leq q \leq 0.009 \ \mathring{\mathbf{A}}^{-1} \ \text{for nominal 60 nm tracers and 0.006}$ $\mathring{\mathbf{A}}^{-1} \leq q \leq 0.017 \ \mathring{\mathbf{A}}^{-1} \ \text{for nominal 20 nm tracers}.$

We also performed complementary event-driven MD simulations to investigate tracer diffusion in aging glass matrices. Fundamental units of σ , m, and $1/k_{\rm B}$ were adopted in the simulations for length, mass, and temperature respectively. The corresponding unit of simulation time is $t_{\rm s} \equiv \sigma (m/k_{\rm B}T)^{1/2}$. The glass matrix was modeled as a 35-component mixture of N = 2048 hard-spheres. ^{48,49} The composition was chosen to yield a discrete normal distribution of particle sizes (mean 1.0, std. 0.1), matching the ca. 10% polydispersity of the experimental system. Similarly, a three-component mixture of hard-sphere tracers with 5%polydispersity was embedded in the matrix at 0.002 volume fraction, resulting in at least 40 tracers per simulation box. The simulations were performed at T = 1, and the mass for matrix particles of average size was set to unity (i.e., m=1), yielding a density $m\sigma^{-3}=1$. Masses of the remaining matrix species and tracers were scaled to obtain the same mass density for each particle in the system. The matrix was compressed in a cubic simulation cell to achieve a final packing fraction $\phi = 0.59$. Simulations at higher volume fractions did not relax on accessible time scales. We note, however, that aging behavior is qualitatively similar for volume fractions above and below the glass transition. ⁵⁰ We correspondingly define $t_{\rm w}$ as the elapsed duration after end of the compression. ^{48,51,52} For each value of $\delta=[0.5,1.2]$ examined, reported results were averaged over at least 72 independent simulations, each initiated from a new matrix configuration. This range of δ was chosen to extend experimental results towards a critical size $\delta_0 = 0.35 \pm 0.05$ associated with anomalous dynamics. 16

Experimentally, the high scattering contrast of the silica tracer particles in x-rays, relative to the other components, ensures that the intensity correlation function g_2 measures the relaxations of tracer particles within the glassy matrix of polystyrene nanoparticles. The experimental g_2 values and those calculated from simulations decay as a function of time and depend on both δ and $t_{\rm w}$ (Fig. 1). To quantify the tracer dynamics, we fit experimental data according to $g_2 = 1 + Bg_1^2 + \varepsilon$, where B is the global experimental contrast related to beam geometry and coherency, $g_1 = A(q) \exp\left[-(t/\tau)^{\beta}\right]$ is the self-intermediate scattering function, A(q) is a wavevector-dependent contrast, β is a positive fitting exponent, and ε captures any residual noise. Because g_2 curves from simulations have less statistical noise, we determine A(q) and $\tau = A(q)/e$ by reading

directly from the individual curves.

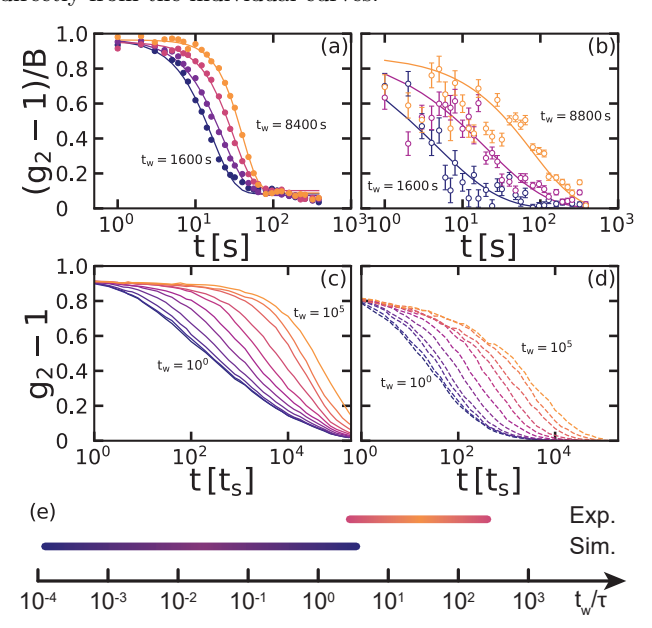


Figure 1. Normalized intensity correlation function $(g_2-1)/B$ at a normalized wavevector $q\sigma=3.5$ as a function of time t for different $t_{\rm w}$. (a,b) Experimental data for tracers of size (a) $\delta=1.65$ and (b) $\delta=0.78$. (c,d) Simulation data for tracers of size (c) $\delta=1$ and (d) $\delta=0.65$. Curves in (a,b) are best fits to stretched exponential functions. (e) Schematic of ratio of waiting time to relaxation time $t_{\rm w}/\tau$ in experiments (yellow) and simulations (blue).

Using simulations and experiments, we measure autocorrelation curves for tracers with various δ across many orders of magnitude in $t_{\rm w}$ (Fig. 1). In simulation, the computational cost of the calculations limits the maximum time scale that can be explored. In experiment, by contrast, the time necessary to load the sample into the beamline places a lower bound on $t_{\rm w}$. Simulation and experiment thus probe complementary ranges of $t_{\rm w}/\tau$ (Fig. 1). As samples age, relaxations in both experiments and simulations become slower, as is common for glassy materials. 53 In experiments, the relaxations of the large tracers ($\delta = 1.65$) are compressed with $\beta > 1$, indicating that these large tracers move hyperdiffusively. Hyperdiffusive relaxations are commonly observed in glassy systems with either attractive or repulsive interactions and are attributed to anisotropic stress relaxations 27,30,35,37,38,54 or to relaxations occurring in regions that are power-law distributed in size. 55,56 In both experiments and simulations, the relaxations of smaller tracers $(\delta < 1.65)$ are stretched with $\beta < 1$ rather than compressed. Experimental g_2 curves for $\delta = 0.78$ are noisier due to lower scattering intensity but still have sufficient signal to noise to quantify tracer dynamics with high reliability. The degree of stretching quantified by β agrees within error for comparably sized tracers in experiments and simulations (Supporting Information). Previous studies 16,20 found that smaller tracers can exhibit fast and anomalous transport. This fast transport arises from size-dependent coupling of hard-sphere tracer dynamics to relaxations of the surrounding glassy matrix, in which the interplay between void diffusion of the tracer particles and slow relaxations of the matrix led to a broad spread of relaxation times.⁵⁷ Thus, the stretched relaxations of small tracer particles likely also reflect coupling to a wider distribution of relaxation modes than are inaccessible to the larger, hyperdiffusive particles. Additionally, as the samples age, the tracer relaxations typically become

less stretched (β increases) in both simulations and experiments (Fig. 1, Supporting Information). The increase in β with increasing $t_{\rm w}$ is consistent with previous work on glassy laponite suspensions ⁴² and suggests that the tracers access a narrower distribution of relaxation modes as the glass ages. ³³

As the samples age, the relaxation times initially increase exponentially for short $t_{\rm w}$ and then transition into a powerlaw increase $\tau \sim t_{\rm w}^n$ with 0 < n < 0.5 at larger $t_{\rm w}$ (Fig. 2). Similar two-step aging processes have been observed for glasses and gels. 27,30,36,50,58,59 In experiments, small tracers relax more slowly than large tracers at large t_w . These slow relaxations likely arise not from the tracer size but rather from small changes in ϕ between samples. Near random close packing, even minor changes in ϕ (Supporting Information) can result in increases in τ of over an order of magnitude. 60 Indeed, τ increases monotonically with tracer size δ in simulations for which ϕ is precisely controlled. Thus, we focus on the qualitative two-step aging mechanism captured in both simulations and experiments. Although the physics underlying the two aging regimes remains poorly understood, one picture proposes that the exponential increase arises from cage formation before entering the power-law full-aging regime. 61-63 Within this long-time aging regime, the power-law exponent n is thought to be related to the deepening and shifting of local minima in the underlying free energy landscape over time. 32,64-66 As the tracer size decreases, n also decreases, indicating that smaller tracers can more easily relax out of these local energy minima and explore the landscape. Additionally, the lower n of small tracers suggest that they may be less spatially localized than larger tracers within the glassy matrix.

Spatial localization manifests as a complex decay in g_2 , with an initial relaxation on very short time scales that corresponds to cage rattling followed by a final relaxation that arises as a particle escapes its localization cage. 67 Although the short-time relaxation occurs on time scales faster than those accessible in experiments, the short-time plateau A(q)in g_2 is less than one for all tracer particles at all t_w (Fig. 3). This suppressed plateau depends on wavevector q, confirming that the tracer particles undergo an initial relaxation within a localization cage. The localization length L_l was extracted from the plateau's q-dependence according to $A(q) = \exp\left[-(L_l q)^2/6\right]$. For experimental measurements, L_l is globally fit across all wavevectors at each waiting time to reduce error associated with determining the intercept for each g_2 curve at a specific q. For simulations, A(q) is extracted directly from the calculated g_2 curves. In both simulation and experiment, L_l does not vary significantly with sample age (Supporting Information) but does depend on particle size (Fig. 4). As particle size increases, L_l decreases monotonically as particles become more strongly caged. The effect of this localization on A(q) depends on the wavevector range over which q_2 is measured. This range is restricted by limitations in scattering intensity in experiments and by computational cost in simulations. Due to these restrictions on the range of accessible wavevectors and to the degree of probe localization, the range of normalized wavevector qL_l is shifted to smaller values for large tracers than it is for small tracers. Thus, even at comparable $q\sigma$, A(q) is more suppressed for small tracers than for large tracers (Fig. 3). Accounting for delocalization at a finite size $\delta_0^{16,20,68,69}$

Accounting for delocalization at a finite size $\delta_0^{16,20,68,69}$ and treating the probe dynamics within a microrheological framework 70,71 so that localization is determined by the elas-

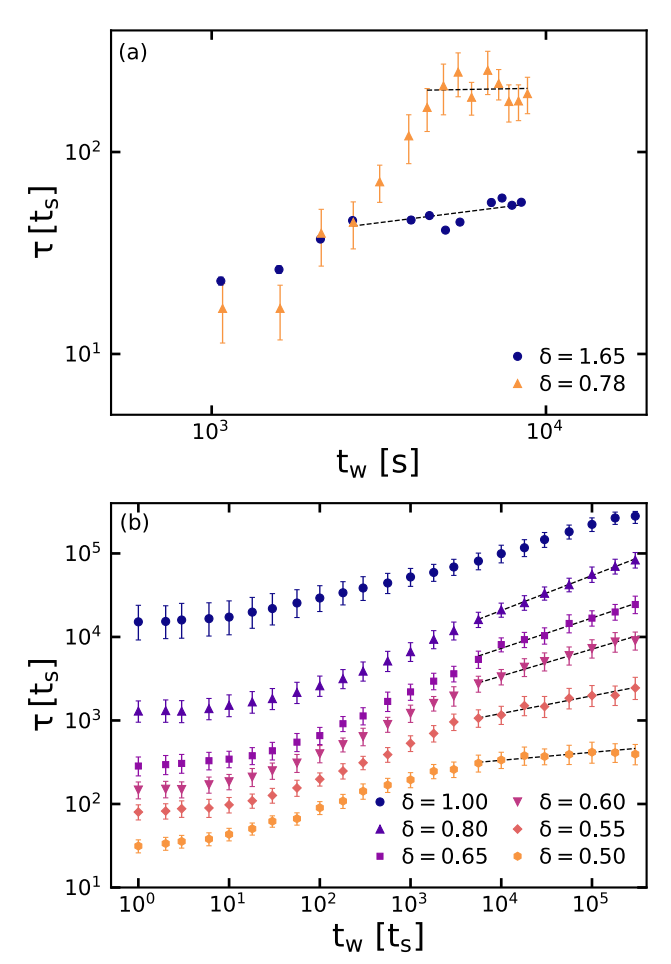


Figure 2. Relaxation time τ at a wavevector $q\sigma=3.5$ as a function of waiting time $t_{\rm w}$ for tracers of different size as measured (a) in experiments and (b) with simulations. Dashed lines are guides to the eye to indicate power-law behaviors.

tic modulus of the matrix, 72,73 the localization length should scale with tracer size as $L_l \sim (\delta - \delta_0)^{-1/2}$ (Supporting Information). The derived scaling behavior cleanly captures the trend in the data with $\delta_0 = 0.38 \pm 0.01$ (inset to Fig. 4). This value of δ_0 is in good agreement with the size ratio at which tracers become delocalized, $\delta \approx 0.35 \pm 0.05$, reported in previous studies on anomalous tracer dynamics in glassy matrices. 16,20 Although electrostatic interactions are present in experiments, the hard-sphere mapping leads to quantitative agreement between simulation and experiment independent of relative sample age $t_{\rm w}/\tau$.

The agreement between the predicted scaling behavior and the measured localization length provides insights into the physics governing tracer transport through glassy matrices. First, delocalization depends not only on the structure of the surrounding matrix but also on the competition between tracer and matrix relaxations. 16,20 Within the resolution of experiments and simulations, L_l does not vary with $t_{\rm w}$ across the range of time scales investigated here (Supporting Information). The lack of a significant aging effect on L_l suggests that the matrix structure, which does not change appreciably with age, may play a larger role in localizing tracer motion than the competition between matrix and tracer relaxations, which both slow with age (Fig. 2). Near delocalization with $\delta \approx \delta_0$, however, the mobility of the matrix is essential for tracers to fully relax out of the

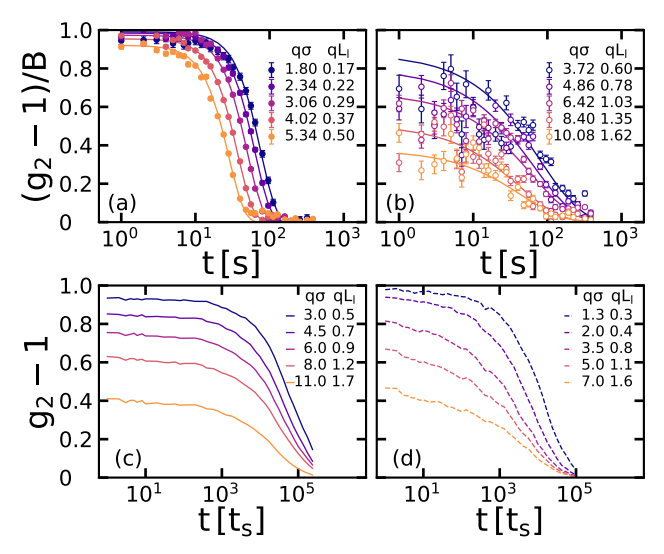


Figure 3. Normalized intensity correlation function $(g_2-1)/B$ as a function of time t for different values of normalized wavevector $q\sigma$. (a,b) Experimental data for tracers of size (a) $\delta = 1.65$ and $t_{\rm w}=8400{\rm s}$ and (b) $\delta=0.78$ and $t_{\rm w}=8800{\rm s}$. (c,d) Simulation data at $t_{\rm w} = 10^5$ for tracers of size (c) $\delta = 1$ and (d) $\delta = 0.65$. Curves in (a,b) are best fits to stretched exponential functions.

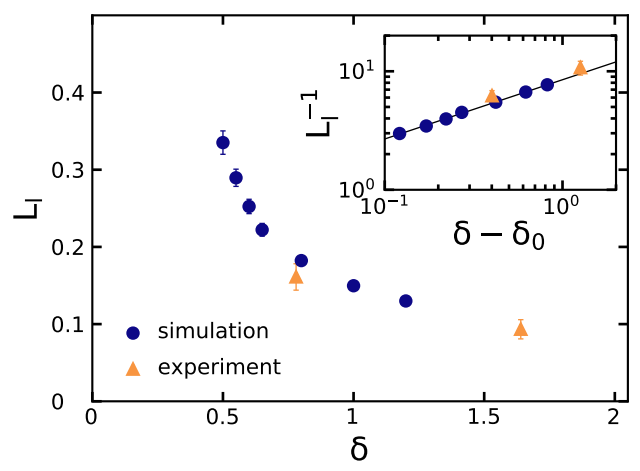


Figure 4. Localization length L_l in units of σ as a function of tracer size δ . Inset: Inverse of localization length as a function of $\delta - \delta_0$, where δ_0 is a critical tracer size at which dynamics become delocalized. Solid curve shows scaling $L_l^{-1} \sim (\delta - \delta_0)^{1/2}$.

transient localization plateau. 16 Second, the agreement between the scaling prediction and observed localization indicates that the relaxations of tracers with $\delta > \delta_0$ are coupled to those of the matrix and thus probe the bulk viscoelasticity of the dense colloidal suspension. This coupling explains the qualitatively similar evolution of tracer and matrix relaxations with $t_{\rm w}$ (Fig. 2).

Our experiments and simulations address how the relative size of tracer particles affect their transport and localization in a glassy matrix. Tracer relaxations are coupled to those of the matrix as the system ages. The tracers become less localized with decreasing size, eventually approaching a delocalization transition at a critical relative size of $\delta_0 \approx 0.38$. The physical picture developed in this work provides direct insight into how particles move and transport through crowded environments with heterogeneous structure and slowly relaxing dynamics, present in materials from cells and tissues to polymer composites to membranes. These findings thus provide a base for predicting particle transport in a wide range of scientifically and industrially relevant processes. Our work addresses localization to matrix structure and dynamics in the simplest case, in which particles interact as pseudo-hard spheres at a single volume fraction. Understanding how this localization transition depends on volume fraction, particle anisotropy, or interparticle interaction strength and range remains poorly understood and should be explored in future studies.

Acknowledgement This research used resources of the Advanced Photon Source, a U.S. Department of Energy (DOE) Office of Science User Facility operated for the DOE Office of Science by Argonne National Laboratory under Contract No. DE-AC02-06CH11357. Support was provided by the National Science Foundation (CBET-1803728, to JCC) and the Welch Foundation (E-1869 to JCC and E-1882 to JCP).

Supporting information available: Static scattering patterns, hard-sphere mapping, fitting parameters τ and β , relaxations of small tracers, simulated tracer mean-squared displacements, derivation of L_l scaling, and L_l vs t_w .

References

- Carpenter, J. F.; Crowe, L. M.; Crowe, J. H. Stabilization of Phosphofructokinase with Sugars during Freeze-Drying: Characterization of Enhanced Protection in the Presence of Divalent Cations. Biochimica et Biophysica Acta 1987, 923, 109 – 115. Cicerone, M. T.; Douglas, J. F. β -Relaxation Governs Protein
- Stability in Sugar-Glass Matrices. Soft Matter 2012, 8, 2983-
- Simo, A.; Polte, J.; Pfänder, N.; Vainio, U.; Emmerling, F.; Rademann, K. Formation Mechanism of Silver Nanoparticles Stabilized in Glassy Matrices. J. Am. Chem. Soc. **2012**, 134, 18824-18833.
- Zhang, K.; Meng, D.; Muller-Plathe, F.; Kumar, S. K. Coarse-Grained Molecular Dynamics Simulation of Activated Penetrant
- Transport in Glassy Polymers. Soft Matter 2018, 440–447. Chang, K.; Korovich, A.; Xue, T.; Morris, W. A.; Madsen, L. A.; Geise, G. M. Influence of Rubbery versus Glassy Backbone Dynamics on Multiscale Transport in Polymer Membranes. Macromolecules 2018, 51, 9222-9233.
- Cai, L.-H.; Panyukov, S.; Rubinstein, M. Mobility of Nonsticky Nanoparticles in Polymer Liquids. Macromolecules 2011, 44, 7853-7863
- Kalathi, J. T.; Yamamoto, U.; Schweizer, K. S.; Grest, G. S.; Kumar, S. K. Nanoparticle Diffusion in Polymer Nanocomposites. Phys. Rev. Lett. 2014, 112, 108301.
- Grabowski, C. A.; Mukhopadhyay, A. Size Effect of Nanoparticle Diffusion in a Polymer Melt. Macromolecules 2014, 47, 7238-
- Poling-Skutvik, R.: Krishnamoorti, R.: Conrad, J. C. Size-Dependent Dynamics of Nanoparticles in Unentangled Polyelec-
- trolyte Solutions. ACS Macro Lett. 2015, 4, 1169–1173. Kumar, S. K.; Benicewicz, B. C.; Vaia, R. A.; Winey, K. I. 50th Anniversary Perspective: Are Polymer Nanocomposites Practical for Applications? Macromolecules 2017, 50, 714–731. Chen, R.; Poling-Skutvik, R.; Nikoubashman,
- Chen, R.; Poling-Skutvik, R.; Nikoubashman, A.; Howard, M. P.; Conrad, J. C.; Palmer, J. C. Coupling of Nanoparticle Dynamics to Polymer Center-of-Mass Motion in Semidilute Polymer Solutions. Macromolecules 2018, 51, 1865 - 1872
- Sorichetti, V.; Hugouvieux, V.; Kob, W. Structure and Dynamics of a Polymer-Nanoparticle Composite: Effect of Nanoparticle Size and Volume Fraction. Macromolecules 2018, 51, 5375-
- Paeng, K.; Park, H.; Hoang, D. T.; Kaufman, L. J. Ideal Probe Single-Molecule Experiments Reveal the Intrinsic Dynamic Heterogeneity of a Supercooled Liquid. Proc. Natl. Acad. Sci. 2015, 112, 4952-4957.
- (14) Heckendorf, D.; Mutch, K. J.; Egelhaaf, S. U.; Laurati, M. Size-Dependent Localization in Polydisperse Colloidal Glasses. Phys.
- Rev. Lett. 2017, 119, 048003.
 Voigtmann, T. Multiple Glasses in Asymmetric Binary Hard Spheres. Europhys. Lett. 2011, 96, 36006.
 Sentjabrskaja, T.; Zaccarelli, E.; De Michele, C.; Sciortino, F.; Tartaglia, P.; Voigtmann, T.; Egelhaaf, S. U.; Laurati, M. Anomalous Dynamics of Intruders in a Crowded Environment of Mobile Obstacles. Nat. Commun. 2016, 7, 11133.
- Zhang, R.; Schweizer, K. S. Correlated Matrix-Fluctuation-Mediated Activated Transport of Dilute Penetrants in Glass-Forming Liquids and Suspensions. J. Chem. Phys. 2017, 146,
- (18) Spanner, M.; Höfling, F.; Schröder-Turk, G. E.; Mecke, K.; Fra-

nosch, T. Anomalous Transport of a Tracer on Percolating Clus-

ters. J. Phys. Condens. Matter 2011, 23, 234120.
Spanner, M.; Höfling, F.; Kapfer, S. C.; Mecke, K. R.; Schröder-Turk, G. E.; Franosch, T. Splitting of the Universality Class of Anomalous Transport in Crowded Media. Phys. Rev. Lett.

2016, *116*, 060601. Roberts, R. C.; Poling-Skutvik, R.; Palmer, J. C.; Conrad, J. C. Tracer Transport Probes Relaxation and Structure of Attractive and Repulsive Glassy Liquids. J. Phys. Chem. Lett. 2018, 9, 3008–3013.

Kim, K.; Miyazaki, K.; Saito, S. Slow Dynamics in Random Media: Crossover from Glass to Localization Transition. *Europhys.* Lett. 2009, 88, 36002.

Kurzidim, J.; Coslovich, D.; Kahl, G. Single-Particle and Collective Slow Dynamics of Colloids in Porous Confinement. Phys. Rev. Lett. **2009**, 103, 138303.

Kurzidim, J.; Coslovich, D.; Kahl, G. Impact of Random Obstacles on the Dynamics of a Dense Colloidal Fluid. *Phys. Rev.* E **2010**, 82, 041505.

Kurzidim, J.; Coslovich, D.; Kahl, G. Dynamic Arrest of Colloids in Porous Environments: Disentangling Crowding and Confinement. J. Phys. Condens. Matter 2011, 23, 234122.

Skinner, T. O. E.; Schnyder, S. K.; Aarts, D. G. A. L.; Horbach, J.; Dullens, R. P. A. Localization Dynamics of Fluids in Random Confinement. *Phys. Rev. Lett.* **2013**, *111*, 128301. Ruta, B.; Chushkin, Y.; Monaco, G.; Cipelletti, L.; Pineda, E.; Bruna, P.; Giordano, V. M.; Gonzalez-Silveira, M. Atomic-Scale

Relaxation Dynamics and Aging in a Metallic Glass Probed by X-Ray Photon Correlation Spectroscopy. Phys. Rev. Lett. 2012, 109, 165701.

Ruta, B.; Pineda, E.; Evenson, Z. Relaxation Processes and Physical Aging in Metallic Glasses. J. Phys. Condens. Matter **2017**, *29*, 503002.

2017, 29, 303002.

Cangialosi, D. Dynamics and Thermodynamics of Polymer Glasses. J. Phys. Condens. Matter 2014, 26, 153101.

Courtland, R. E.; Weeks, E. R. Direct Visualization of Ageing in Colloidal Glasses. J. Phys. Condens. Matter 2003, 15, S359.

Cipelletti, L.; Manley, S.; Ball, R. C.; Weitz, D. A. Universal Aging Features in the Restructuring of Fractal Colloidal Gels. Phys. Rev. Lett. 2000, 87, 2275–2278.

Phys. Rev. Lett. **2000**, 84, 2275–2278.

McKenna, G. B.; Narita, T.; Lequeux, F. Soft Colloidal Matter: A Phenomenological Comparison of the Aging and Mechanical Responses with Those of Molecular Glasses. J. Rheol. **2009**, 53,

Kob, W.; Barrat, J.-L. Aging Effects in a Lennard-Jones Glass. *Phys. Rev. Lett.* **1997**, *78*, 4581–4584. Cloitre, M.; Borrega, R.; Leibler, L. Rheological Aging and Review of the control of the contr

juvenation in Microgel Pastes. Phys. Rev. Lett. 2000, 85, 4819-

Yunker, P.; Zhang, Z.; Aptowicz, K. B.; Yodh, A. G. Irreversible

Rearrangements, Correlated Domains, and Local Structure in Aging Glasses. *Phys. Rev. Lett.* **2009**, *103*, 115701.

Bouzid, M.; Colombo, J.; Barbosa, L. V.; Del Gado, E. Elastically Driven Intermittent Microscopic Dynamics in Soft Solids.

Nat. Commun. 2017, 8, 15846.
Bellour, M.; Knaebel, A.; Harden, J. L.; Lequeux, F.;
Munch, J. P. Aging Processes and Scale Dependence in Soft

Glassy Colloidal Suspensions. *Phys. Rev. E.* **2003**, *67*, 8. Cipelletti, L.; Ramos, L.; Manley, S.; Pitard, E.; Weitz, D. A.; Pashkovski, E. E.; Johansson, M. Universal Non-Diffusive Slow Dynamics in Aging Soft Matter. *Faraday Discuss.* **2003**, *123*,

Bandyopadhyay, R.; Liang, D.; Yardimci, H.; Sessoms, D. A.; Borthwick, M. A.; Mochrie, S. G. J.; Harden, J. L.; Leheny, R. L. Evolution of Particle-Scale Dynamics in an Aging Clay Suspension. *Phys. Rev. Lett.* **2004**, *93*, 228302.
Cianci, G. C.; Courtland, R. E.; Weeks, E. R. Correlations of

Ctructure and Dynamics in an Aging Colloidal Glass. Solid State

Communications 2006, 139, 599 – 604. Lynch, J. M.; Cianci, G. C.; Weeks, E. R. Dynamics and Structure of an Aging Binary Colloidal Glass. Phys. Rev. E. 2008, 78. 031410.

Kaloun, S.; Skouri, R.; Skouri, M.; Munch, J. P.; Schosseler, F. Successive Exponential and Full Aging Regimes Evidenced by Tracer Diffusion in a Colloidal Glass. *Phys. Rev. E* **2005**, *72*,

Schosseler, F.: Kaloun, S.: Skouri, M.: Munch, J. P. Diagram of the Aging Dynamics in Laponite Suspensions at Low Ionic Strength. *Phys. Rev. E* **2006**, *73*, 021401. Strachan, D. R.; Kalur, G. C.; Raghavan, S. R. Size-Dependent

Diffusion in an Aging Colloidal Glass. Phys. Rev. E 2006, 73,

(44) Levitz, P.; Lecolier, E.; Mourchid, A.; Delville, A.; Lyonnard, S. Liquid-Solid Transition of Laponite Suspensions at Very

Low Ionic Strength: Long-Range Electrostatic Stabilisation of Anisotropic Colloids. Europhys. Lett. 2000, 49, 672.

Van Megen, W.; Pusey, P. N. Dynamic Light-Scattering Study of the Glass Transition in a Colloidal Suspension. Phys. Rev. A

1991, 43, 5429-5441.
Park, N.; Conrad, J. C. Phase Behavior of Colloid-Polymer Depletion Mixtures with Unary or Binary Depletants. Soft Matter

2017, 13, 2781–2792.
Poon, W. C. K.; Weeks, E. R.; Royall, C. P. On Measuring Colloidal Volume Fractions. Soft Matter 2012, 8, 21–30.

(48) Zaccarelli, E.; Liddle, S. M.; Poon, W. C. On Polydispersity and the Hard Sphere Glass Transition. Soft Matter 2015, 11,

(49) Zaccarelli, E.; Valeriani, C.; Sanz, E.; Poon, W.; Cates, M.; Pusey, P. Crystallization of Hard-Sphere Glasses. *Phys. Rev. Lett.* 2009, 103, 135704.

El Masri, D.; Berthier, L.; Cipelletti, L. Subdiffusion and Intermittent Dynamic Fluctuations in the Aging Regime of Concentrated Hard Spheres. *Phys. Rev. E* **2010**, *82*, 031503. Puertas, A. M. Aging of a Hard-Sphere Glass: Effect of the

Microscopic Dynamics. J. Phys. Condens. Matter 2010, 22, 104121.

Foffi, G.; Zaccarelli, E.; Buldyrev, S.; Sciortino, F.; Tartaglia, P. Aging in Short-Ranged Attractive Colloids: A Numerical Study.

Aging in Short-Ranged Attractive Colloids: A Numerical Study. J. Chem. Phys. **2004**, 120, 8824–8830. Zhao, J.; Simon, S. L.; McKenna, G. B. Using 20-Million-Year-Old Amber to Test the Super-Arrhenius Behaviour of Glass-Forming Systems. Nat. Commun. **2013**, 4, 1783. Ramos, L.; Cipelletti, L. Ultraslow Dynamics and Stress Relaxation in the Aging of a Soft Glassy System. Phys. Rev. Lett. **2001**, 87, 245503.

2001, 87, 245503.

(55) Rogers, M. C.; Chen, K.; Andrzejewski, L.; Narayanan, S.; Ramakrishnan, S.; Leheny, R. L.; Harden, J. L. Echoes in X-ray Speckles Track Nanometer-Scale Plastic Events in Colloidal Gels Under Shear. Phys. Rev. E **2014**, 90, 062310.

Conder Snear. Phys. Rev. E 2014, 90, 002310.

Rogers, M. C.; Chen, K.; Pagenkopp, M. J.; Mason, T. G.; Narayanan, S.; Harden, J. L.; Leheny, R. L. Microscopic Signatures of Yielding in Concentrated Nanoemulsions Under Large-Amplitude Oscillatory Shear. Phys. Rev. Mater. 2018, 2, 002302. 095601

Laurati, M.; Sentjabrskaja, T.; Ruiz-Franco, J.; Egelhaaf, S. U.; Zaccarelli, E. Different Scenarios of Dynamic Coupling in Glassy Colloidal Mixtures. Phys. Chem. Chem. Phys. 2018, 20, 18630-

Guo, H.; Ramakrishnan, S.; Harden, J. L.; Leheny, R. L. Gel Formation and Aging in Weakly Attractive Nanocolloid Suspen-sions at Intermediate Concentrations. *J. Chem. Phys.* **2011**, 135, 154903.

Angelini, R.; Zulian, L.; Fluerasu, A.; Madsen, A.; Ruocco, G.; Ruzicka, B. Dichotomic Aging Behaviour in a Colloidal Glass

кылика, В. Dicnotomic Aging Behaviour in a Colloidal Glass. Soft Matter 2013, 9, 10955. Cheng, Z.; Zhu, J.; Chaikin, P. M.; Phan, S.-E.; Russel, W. B. Nature of the Divergence in Low Shear Viscosity of Colloidal Hard-Sphere Dispersions. Phys. Rev. E. 2002, 65, 041405. Bonn, D.; Tanaka, H.; Wegdam, G.; Kellay, H.; Meunier, J. Aging of a Colloidal "Wigner" Glass. Europhys. Lett. 1999, 45, 52–57.

Bonn, D.; Kellay, H.; Tanaka, H.; Wegdam, G.; Meunier, J. Laponite: What is the Difference Between a Gel and a Glass? Langmuir **1999**, 15, 7534–7536.

Tanaka, H.; Jabbari-Farouji, S.; Meunier, J.; Bonn, D. Kinetics of Ergodic-to-Nonergodic Transitions in Charged Colloidal Suspensions: Aging and Gelation. *Phys. Rev. E.* **2005**, *71*, 1–10. Utz, M.; Debenedetti, P. G.; Stillinger, F. H. Atomistic Simu-

lation of Aging and Rejuvenation in Glasses. Phys. Rev. Lett. **2000**, *84*, 1471–1474.

Bouchaud, J. P. Soft Fragile Matter Nonequilibrium Dyn.

Metastability, Flow; 2000; pp 285–304.
Lubchenko, V.; Wolynes, P. G. Theory of Aging in Structural Glasses. J. Chem. Phys. 2004, 121, 2852–2865.
Joshi, Y. M. Dynamics of Colloidal Glasses and Gels. Annu.

Rev. Chem. Biomol. Eng. 2014, 5, 181–202.
Thakur, J. S.; Bosse, J. Glass Transition of Two-Component Liquids. I. The Debye-Waller Factors. Phys. Rev. A 1991, 43, 4378 - 4387

Thakur, J. S.; Bosse, J. Glass Transition of Two-Component Liquids. II. The Lamb-Mössbauer Factors. *Phys. Rev. A* **1991**, *3*, 4388–4395.

Mason, T. G.; Weitz, D. A. Optical Measurements of Frequency-Dependent Linear Viscoelastic Moduli of Complex Fluids. *Phys. Rev. Lett.* **1995**, *74*, 1250–1253.

Squires, T. M.; Mason, T. G. Fluid Mechanics of Microrheology. *Annu. Rev. Fluid Mech.* **2010**, *42*, 413–438.

Mason, T. G.; Weitz, D. A. Linear Viscoelasticity of Colloidal Hard Sphere Suspensions Near the Glass Transition. Phys. Rev.

Lett. 1995, 75, 2770–2773. Greinert, N.; Wood, T.; Bartlett, P. Measurement of Effective Temperatures in an Aging Colloidal Glass. Phys. Rev. Lett. **2006**, *97*, 265702.